ENABLING HIGH-ENERGY/HIGH-VOLTAGE LITHIUM-ION CELLS FOR TRANSPORTATION: THEORY AND MODELING

Project ID: BAT253

HAKIM IDDIR

Argonne National Laboratory
June 19,2018

2018 DOE Vehicle Technologies Office Annual Merit Review

OVERVIEW

Timeline

- Start: October 1, 2014
- End: Sept. 30, 2018
- Percent complete: 94%

Budget

- Total project funding:
  FY17 $4.0M
- BAT252, BAT253, and BAT254 (ANL, NREL, ORNL, LBNL)

Barriers

- Development of PHEV and EV batteries that meet or exceed DOE and USABC goals
  - Cost
  - Performance
  - Safety

Partners

- Oak Ridge National Laboratory
- National Renewable Energy Laboratory
- Lawrence Berkeley National Laboratory
- Argonne National Laboratory

PROJECT OBJECTIVES - RELEVANCE

Gain understanding of the atomic-scale processes that influence the structure and stability of NMC surfaces under various electrochemical environments

MILESTONES

- Determination of surface structures and the driving force for surface elemental segregation
- Theoretical predictions of electrolyte and additive-NMC surface interactions
- Theoretical predictions of electrolyte decomposition and dissolution products
- Understanding of coating structures, surface reconstructions, and influence on elemental segregation

APPROACH

ATOMISTIC MODELING

- Spin-polarized density functional theory (DFT)
- Generalized gradient approximation (GGA) parametrized by Perdew, Burke, and Ernzerholf (PBE).
- The GGA+U scheme is used for applying the on-site correlation effects among 3d electrons of the transition metals (TM)
- After geometry optimizations within the DFT+U framework, electronic relaxation was performed using a single point calculation with the hybrid functional HSE06
- Bulk solvent effects were accounted for by using an implicit solvation (VASPsol)
- Calculations in solution were performed using Gaussian09 with the M062X functional, 6-311+G(d,p) basis set and the CPCM solvent model

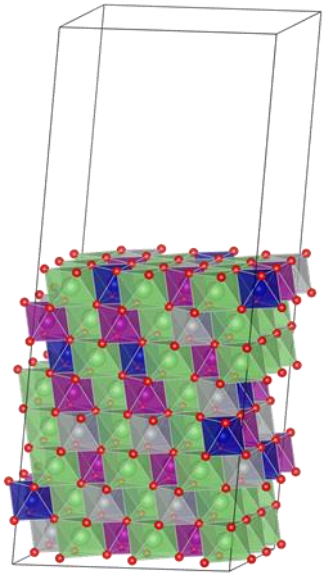

Periodic boundary conditions (slab models)

ELECTROCHEMICAL MODELING

- In general, the electrochemical modeling activities build on earlier successful characterization and modeling studies in extending efforts to high-energy and high-voltage lithium ion systems.
  - Present focus is on electrode side reactions and crosstalk between electrodes.

MOST RELEVANT NMC FACETS

Surface energy of (012) facet as a function of the oxygen chemical potential (NMC111)

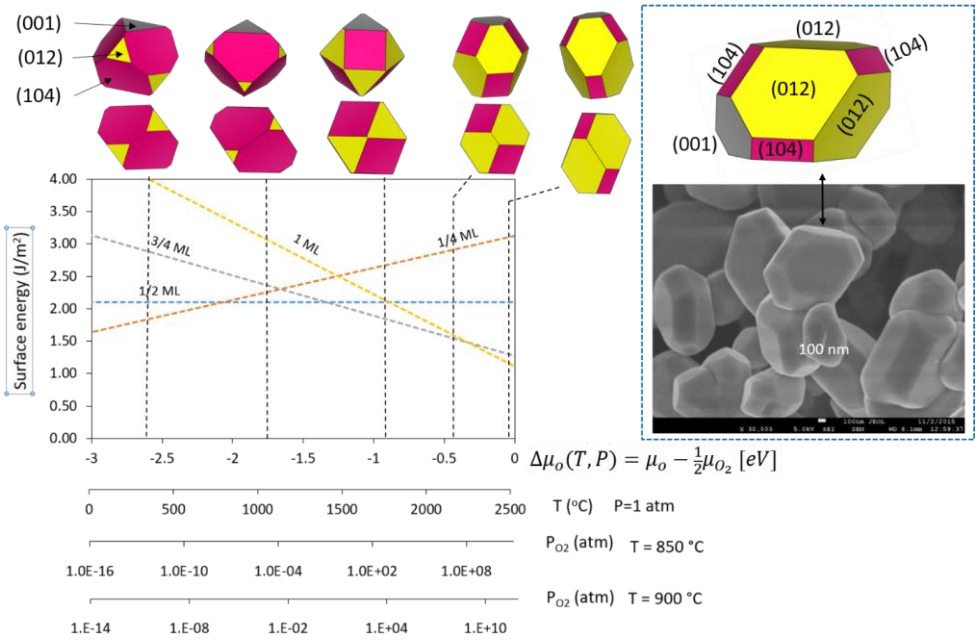

Surface energy of the (001) facet as a function of the Li chemical potential (NMC111)

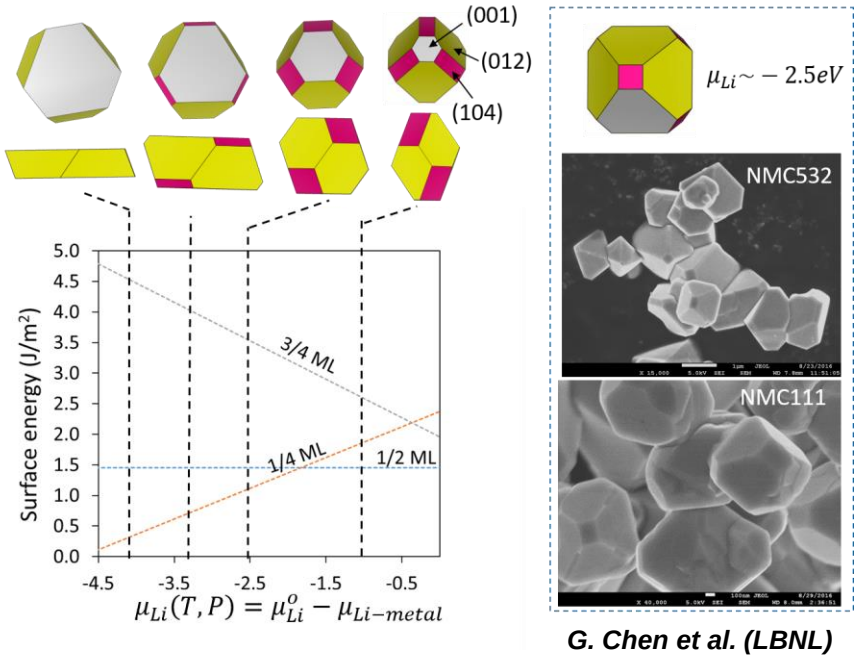

G. Chen et al. (LBNL)

- The (012) surface is predominant (>80% of total surface area)
- This facet is used as the prototype surface in our models

Predicted particle shapes, surface activity and stability verified by experiments

SYNTHESIS OF SURFACE-SPECIFIC NMC SINGLE CRYSTALS

G. Chen et al. (LBNL)

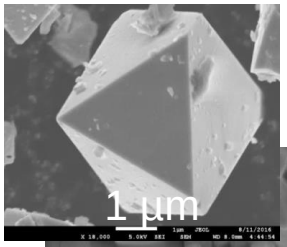

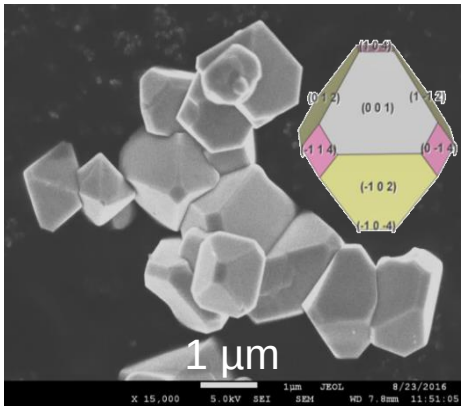

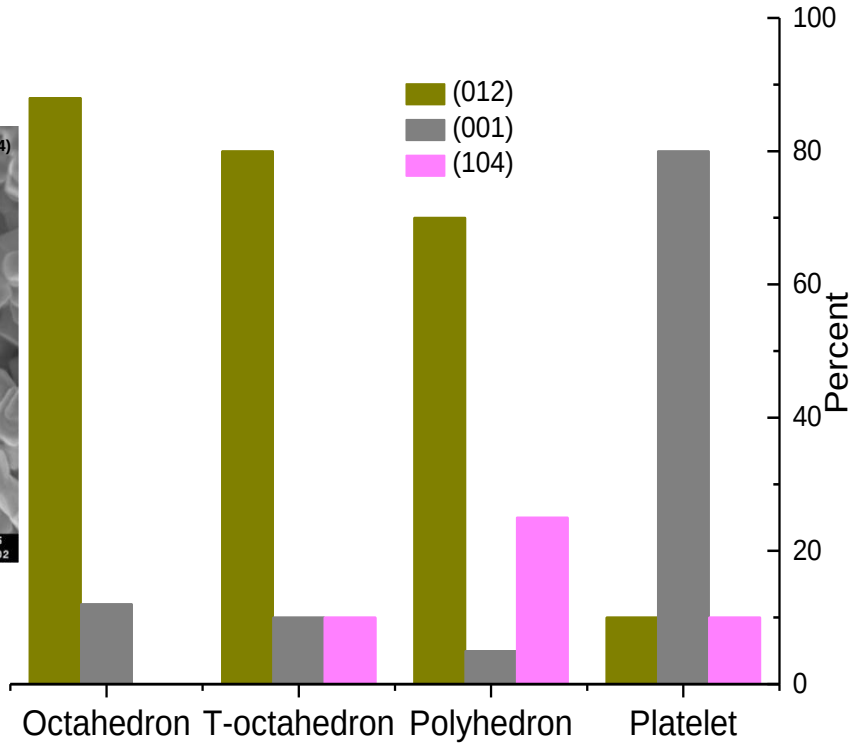

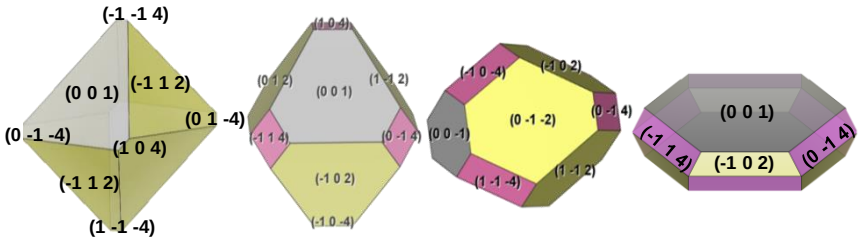

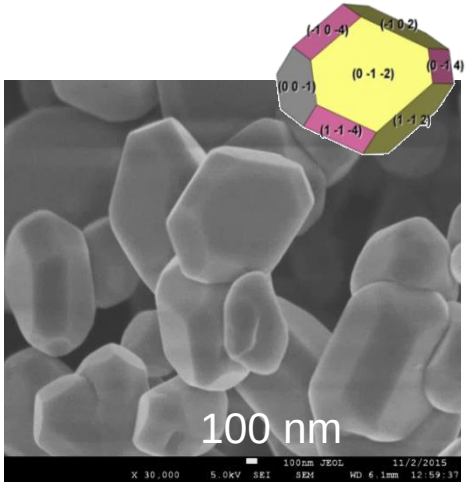

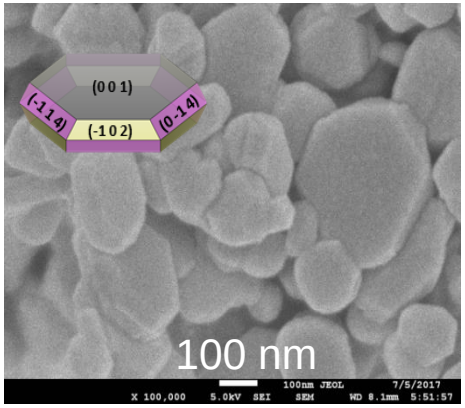

OAK RIDGE National Laboratory

NREL NATIONAL RENEWABLE ENERGY LABORATORY

BERKELEY LAB

Argonne NATIONAL LABORATORY

EXPERIMENT CONFIRMS PREDICTED TRENDS

NMC333

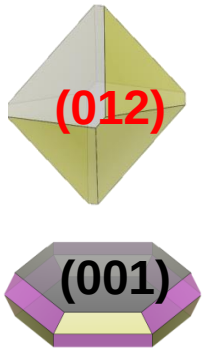

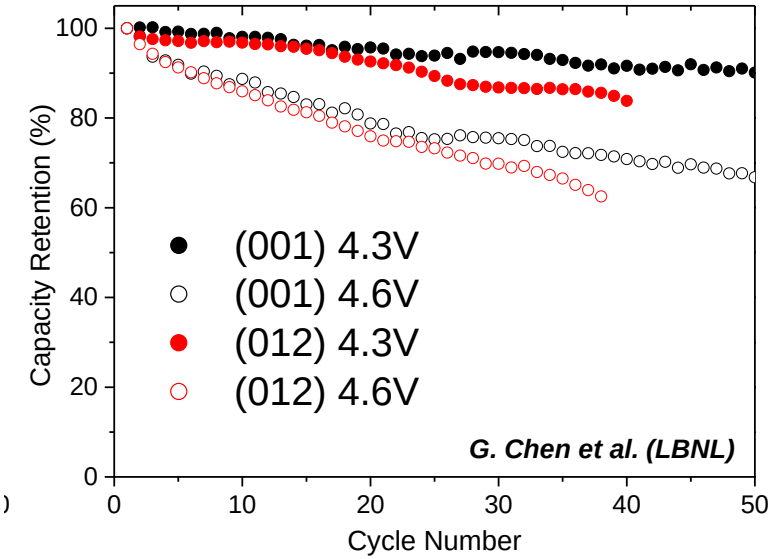

- Same composition (NMC333), same size (~200 nm) and same voltage window.
- Sample with (012) surface outperforms (001) surface in initial capacity but (001) sample has better cycling stability.

Pristine NMC has surface-dependent surface reconstruction layers (SRL)

R. Shahbazian-Yassar, S. Sharifi Asl (UIC)

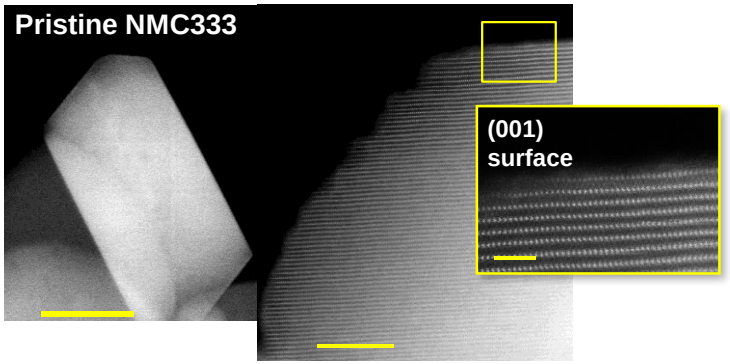

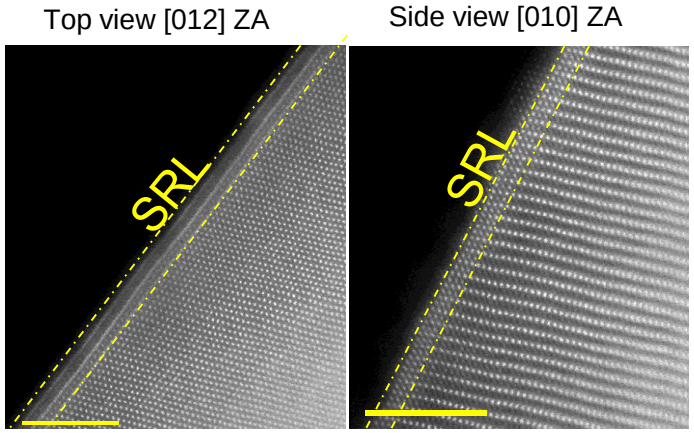

- Typical surface reconstruction layer (SRL) on pristine NMC333 is ~1 nm.
- Formation of SRL facet dependent – no SRL seen on pristine (001) surface of NMC333.

Co SURFACE SEGREGATION TO (104) FACET

Co PDOS d orbitals

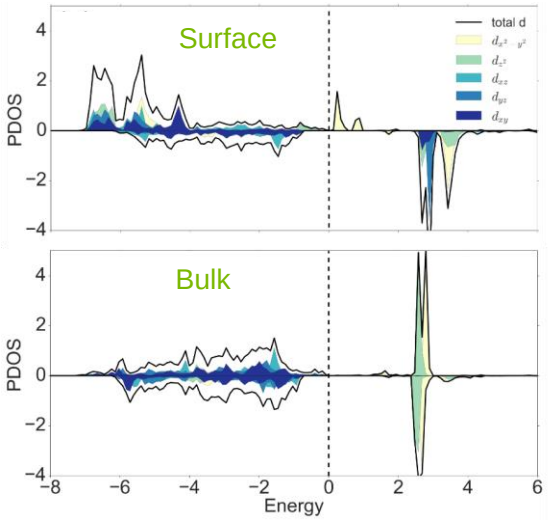

d orbitals occupancy

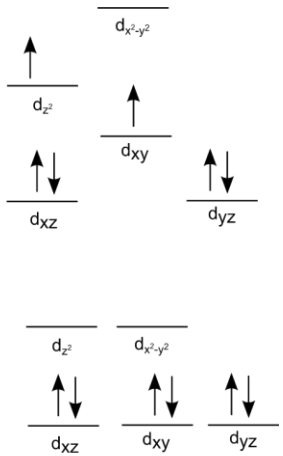

- Bulk: unoccupied states and the magnetization is zero, indicating Co^{3+} in the low spin configuration.
- The crystal field splitting energy is less than the spin pairing energy (P) → the low spin configuration is favored.
- Surface: magnetization, Bader charges, and PDOS analysis indicates Co^{3+} in an intermediate spin state.
- The crystal field splitting energy < P

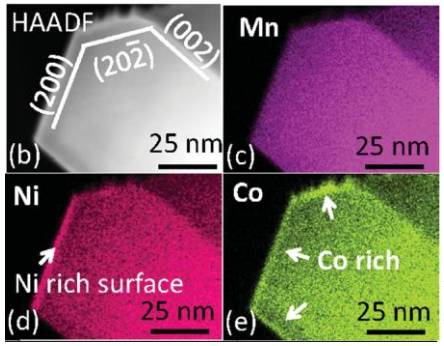

Yan, P.; et. Al. *Adv. Energy Mater.* **2016**, *6* (9), 1502455.

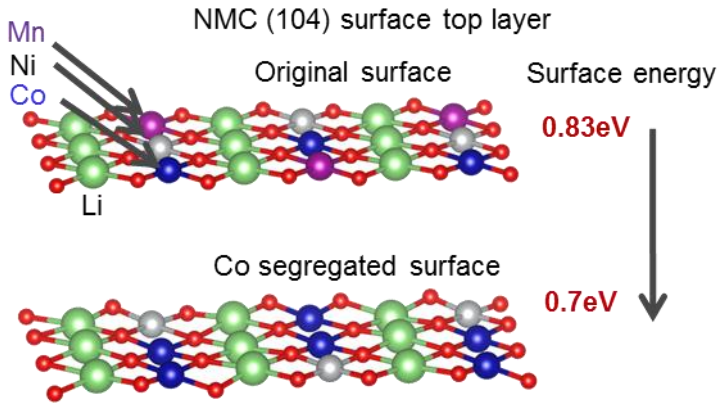

The stability of intermediate spin state Co ions at the (104) NMC111 surface produces a thermodynamic driving force for segregation

FACET-DEPENDENT Ni SEGREGATION

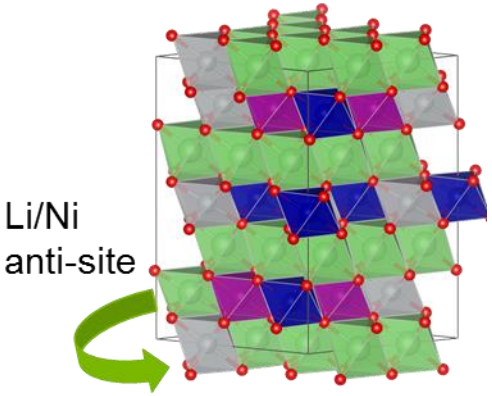

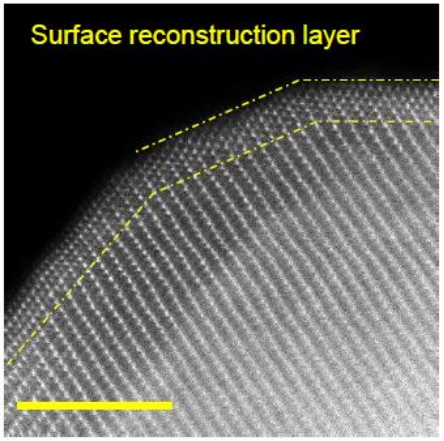

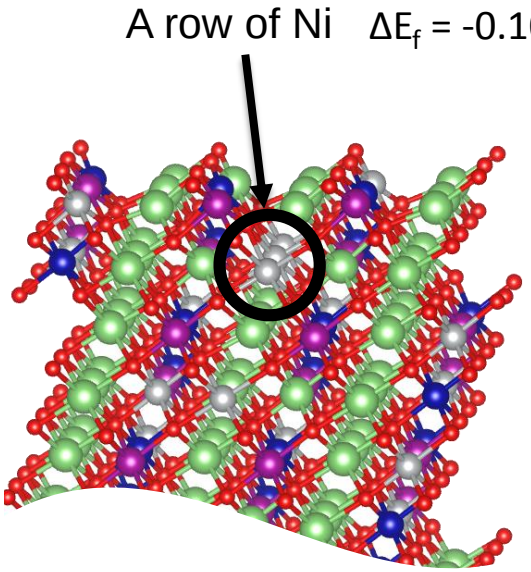

- Bulk Li/Ni anti-site defect formation energy is $E_f \approx 0.3eV$ → equilibrium concentration:

$$C = N_{conf} e^{\frac{-E_f}{RT}}$$ → 1.3% @ T = 298.15 K

- The anti-site defect formation energy is independent on its distance to the surface
- The formation energy of a row of anti-site defect near the surface is slightly negative
- There is a driving force to form a spinel-like top layer in the fully lithiated (012) NMC111 surface
- The results suggest a mechanism for Ni migration and phase transformation near the surface

Li-Ni exchange and Ni migration to the surface is at the origin of the surface reconstruction

STRAIN DRIVEN SPINEL STABILIZATION AT THE (012) SURFACE

The reconstructed surface is pinned to the unit cell of the particle

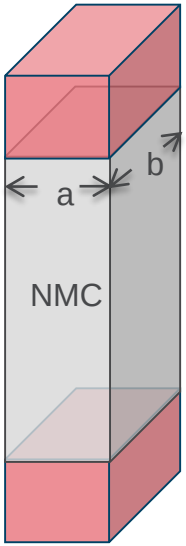

(a and b fixed to NMC111)

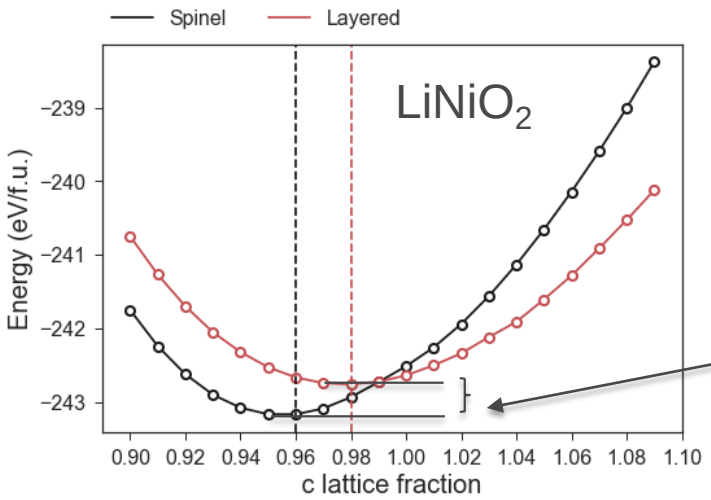

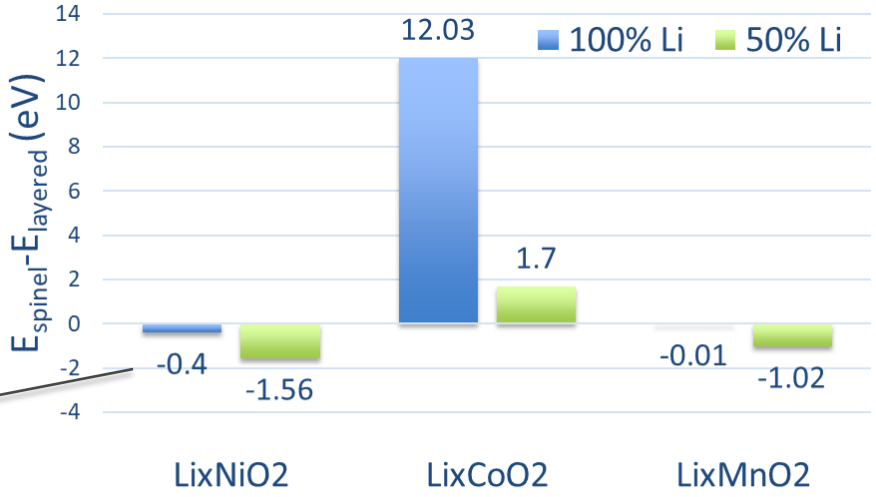

R. Shahbazian-Yassar, S. Sharifi Asl (UIC)

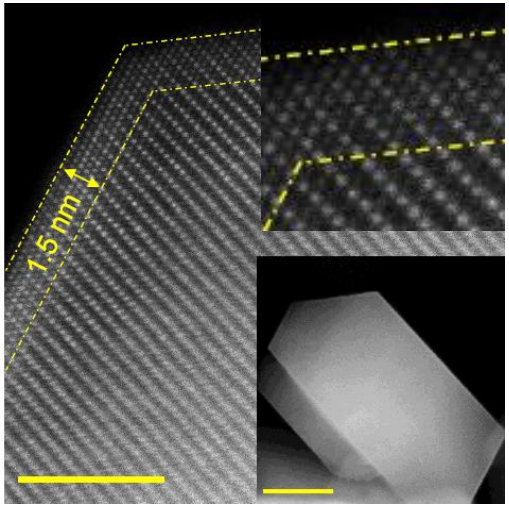

- $LiNiO_2$ and $LiMnO_2$ spinel-like phases are more stable than the layered phases when the phase is pinned to the NMC lattice.
- More Li-Ni exchange than Li-Mn exchange → Ni-rich surface reconstruction.

There is a driving force for Ni to segregate to the surface and reconstruct to a spinel-like phase

FLUORINATED VS NON-FLUORINATED ELECTROLYTES

See BAT252

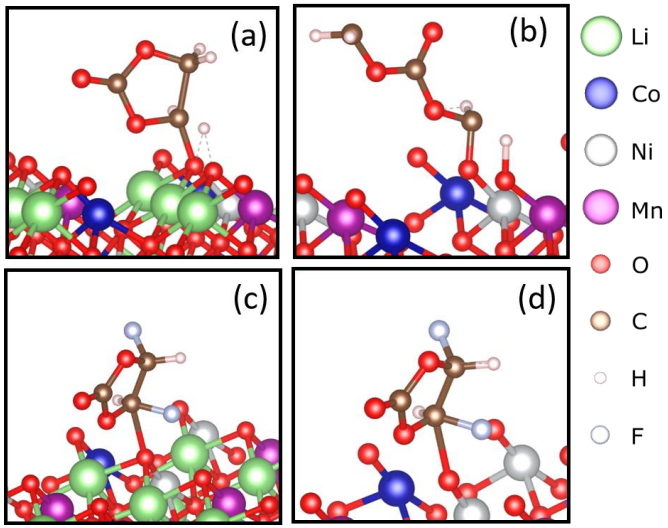

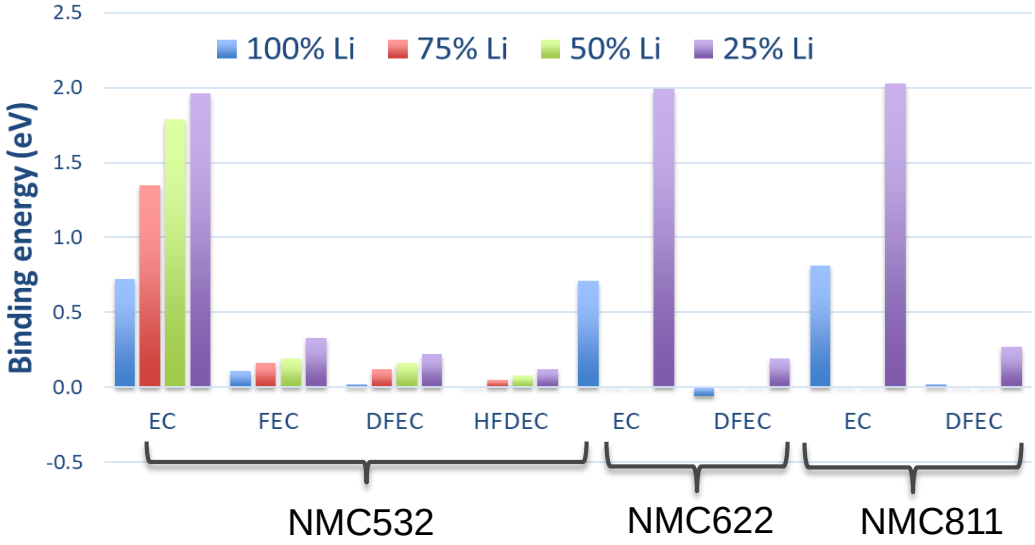

(a) EC on a lithiated (012) surface
(b) EC on a delithiated (012) surface
(c) DFEC on a lithiated (012) surface.
(d) DFEC on a delithiated (012) surface.

EC oxidation $\Delta E_b = -2.3eV$

DFEC oxidation is not favorable

- Fluorinated compositions: FEC, DFEC and HFDEC present weaker interactions with the NMC surfaces.
- Adsorption/reaction energies of fluorinated molecules are much smaller than that for EC → less decomposition of fluorinated compositions is expected. EC would decompose preferentially, since it competes favorably for the adsorption sites.
- The trend in binding energies is independent of Ni content in the transition metal layer

Limited cathode surface reconstructions/transformations are expected with the fluorinated electrolytes compared to the non-fluorinated electrolytes

NMC SURFACE-PHOSPHITE ADDITIVES INTERACTION

See BAT252

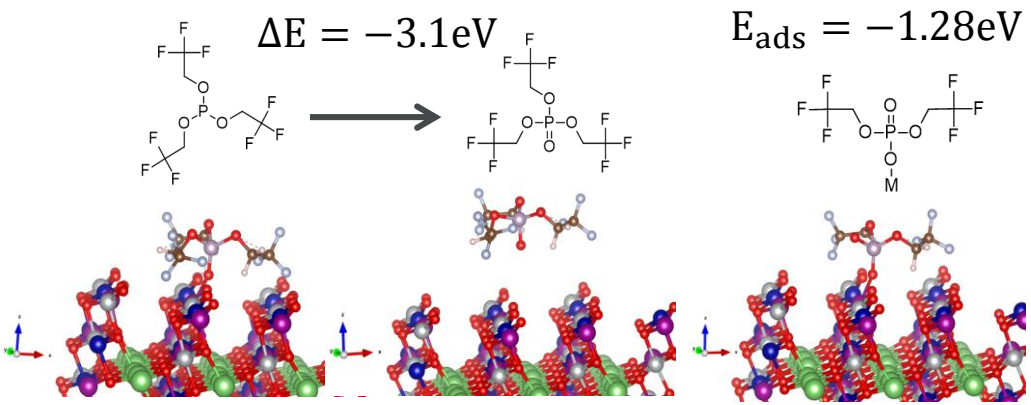

- CH_2CF_3 groups of TTFP do not impede P-O interaction at the surface
- The molecule is easily oxidized to TMSPa
- If TTFP loses a CH_2CF_3 group the product is stable at the surface.

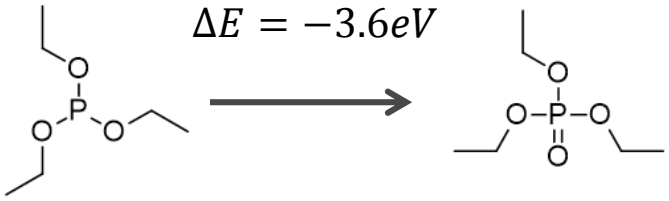

- TEPi is oxidized to TEPa at the surface.
- No stable species at the surface (no surface passivation)

The strength of the interaction depends on the functional groups in the phosphite an the degree of decomposition of the additive

AGING OF TMSPI MITIGATES IMPEDANCE RISE

See BAT252

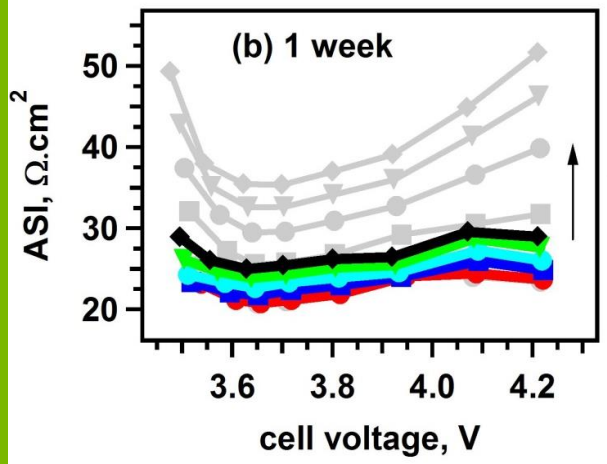

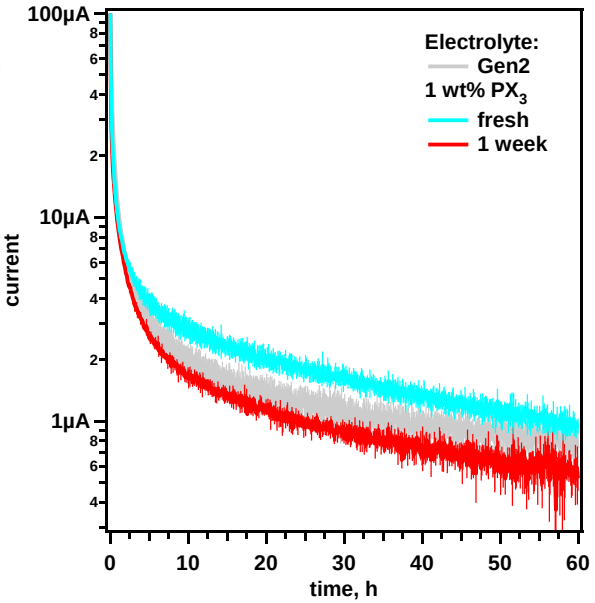

- ASI plot for aged (1 week) electrolyte containing 1 wt% TMSPi (color lines).
- The grey lines indicate the baseline electrolyte tested using identical cycling and HPPC protocols.

- Current vs. time potentiostatic hold at 4.6 V vs Li/Li^{+}.
- Baseline electrolyte (black line) 1 wt% PX_3 before (blue line) and after one week of ex-situ aging (red line).
- 1 week old →lowest oxidation current

- TMSPi interaction with the surface is weak due to bulky TMS groups
- TMSPi can lose a TMS group and form a phosphate on the surface
- The phosphate adsorbs favorably on the surface

$E_{ads} = -0.08eV$ $E_{ads} = -1.2eV$

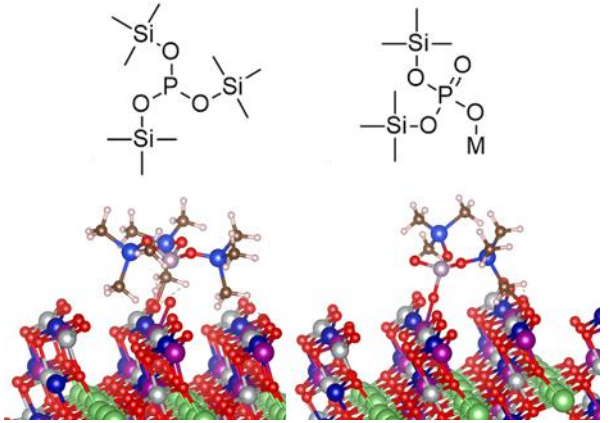

TMSPi decomposition products passivate the surface

TMSPI DECOMPOSITION TIMELINE: AGING

See BAT252

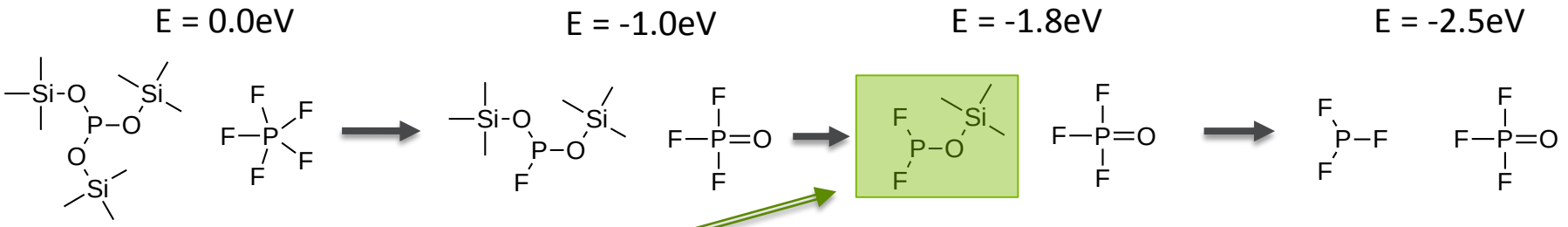

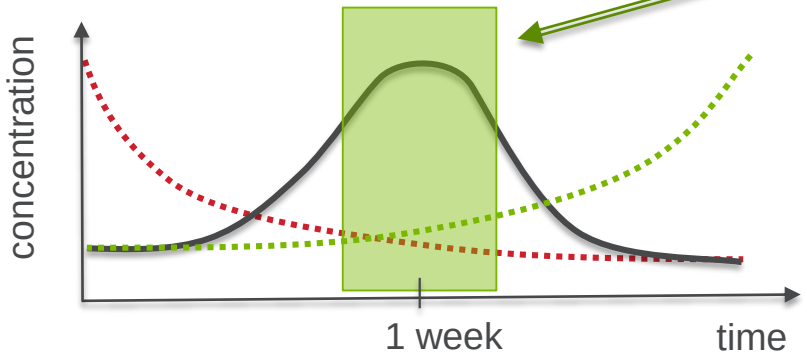

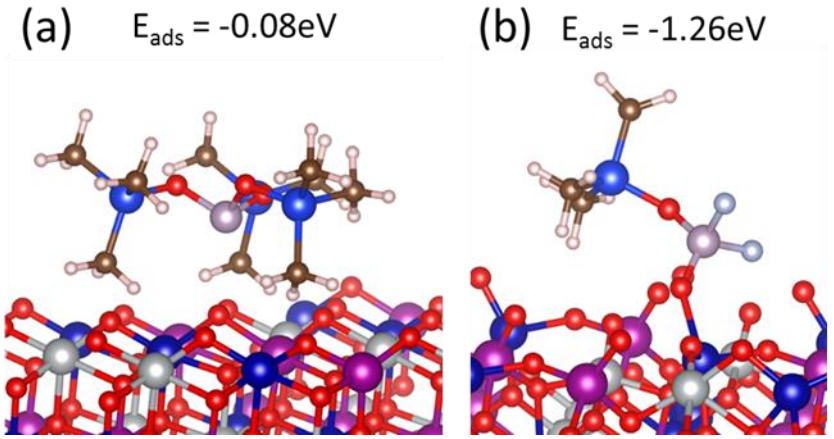

Molecular configuration for chemisorbed (a) PX3 and (b) PF2X molecules on partially delithiated NMC.

- TMSPi decomposition to PF_3 route is favorable.
- Reaction with PF_5 is favored after the first decomposition step (first reaction step with HF is more favorable than with PF_5).

Surface passivation by the partially decomposed TMSPi

- TMSPi (PX_3) has a weak interaction with the surface while PF_2X (1 branch) molecules interact strongly with the surface (chemisorption, surface passivation).

LiACAC SALT IS ABLE TO DISSOLVE THE TM WITHOUT OXIDATION/REDUCTION REACTIONS

See BAT252

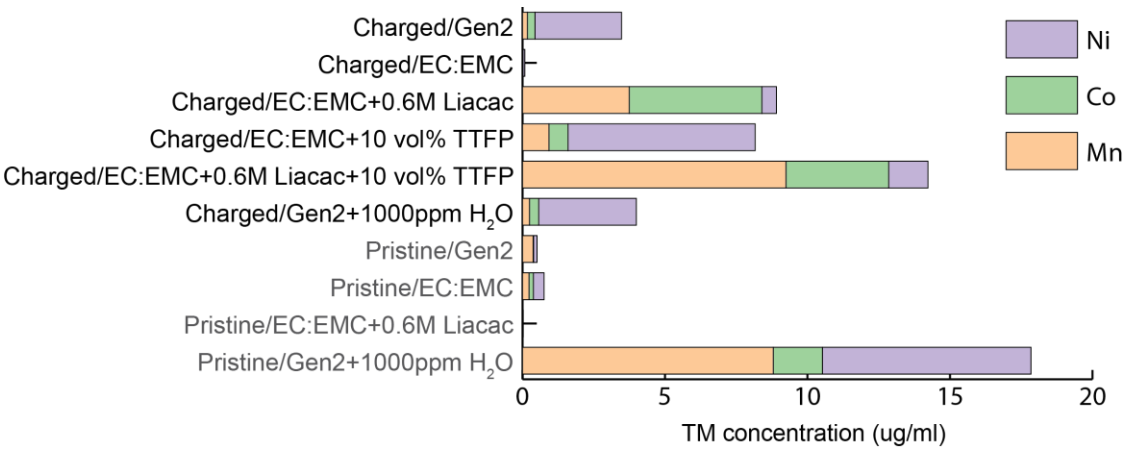

Transition metal dissolution in the absence of LiACAC

- In the charged state, Ni cations are first to be reduced → More Ni dissolution in charged state.
- In the pristine state, Mn cations are first to be reduced → More Mn dissolution in pristine state.

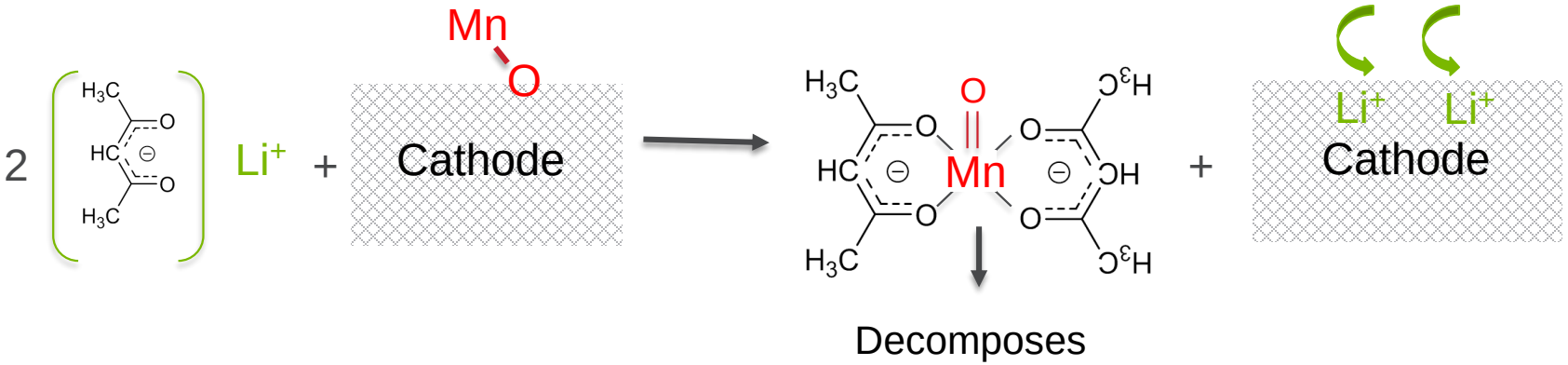

Mn-oxo complex intermediates contribute to Mn dissolution without oxidation of the solvent

See BAT254

α-$LiAlO_2$ BUFFER COATING ON NMC

- α-LiAlO2 / NMC interface formation energy is very low ~ 0.1eV/f.u.
- γ-LiAlO2 / NMC does not form a simple interface (symmetry considerations).

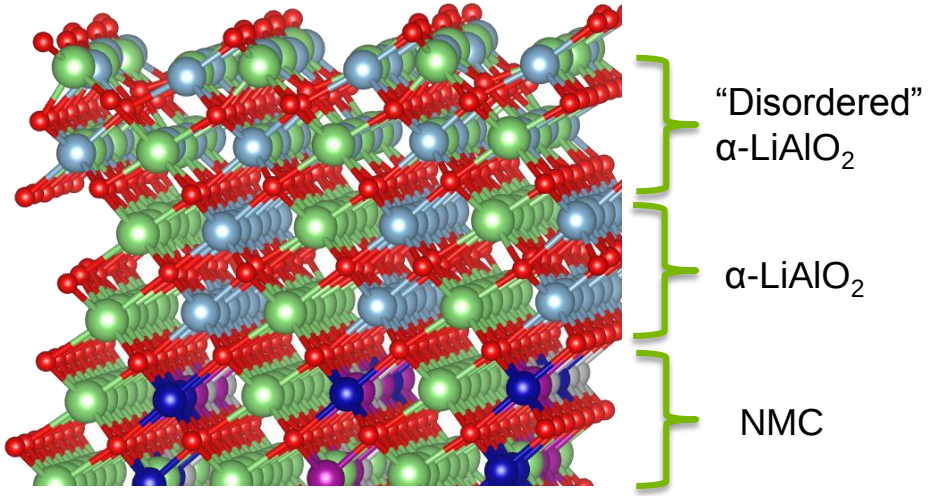

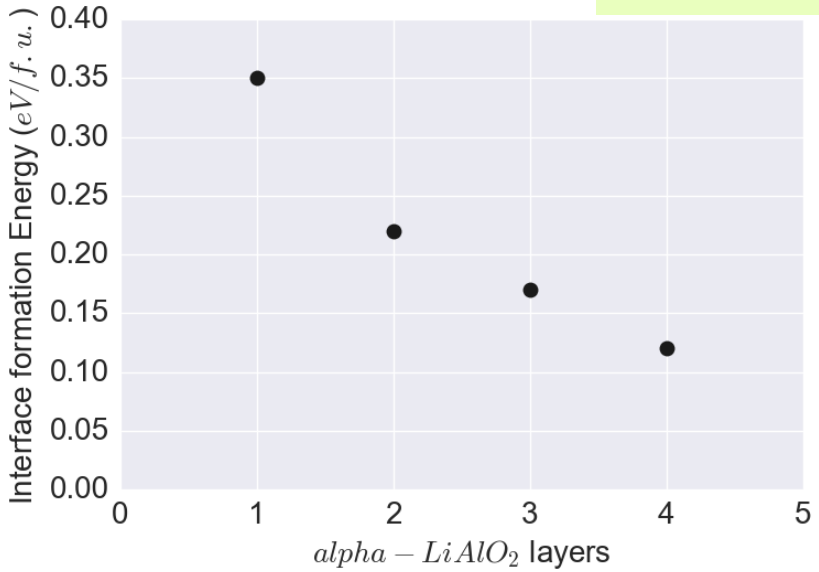

Interface Energy = $E_{LiAlO2\_slab} + E_{NMC\_Bulk} - E_{LiAlO2/NMC}$

- α-LiAlO2 / "disordered-α-LiAlO2" interface makes the α-LiAlO2 /NMC less favorable.
- 4 α-LiAlO2 layers or more compensates the effect of the disordered phase.

A thin buffer α-$LiAlO_2$ phase between γ-$LiAlO_2$ and NMC (012) surface is predicted

ALUMINA EFFECT ON METAL SEGREGATION

See BAT254

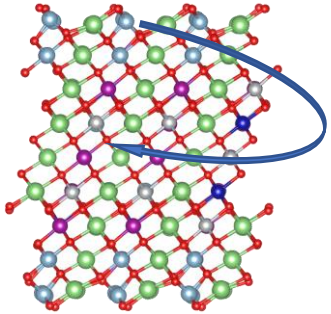

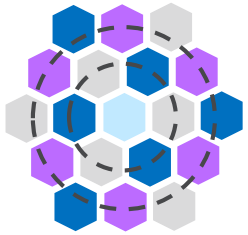

Specie swapped	AlO_2/NMC111 ΔE (eV)	$LiAlO_2$/NMC111 ΔE (eV)	AlO_2/$Li(M)O_2$ ΔE (eV)
Co	1.63	-0.02	0.95
Ni	0.21	-0.33	0.03
Mn	-1.02	0.42	-0.52

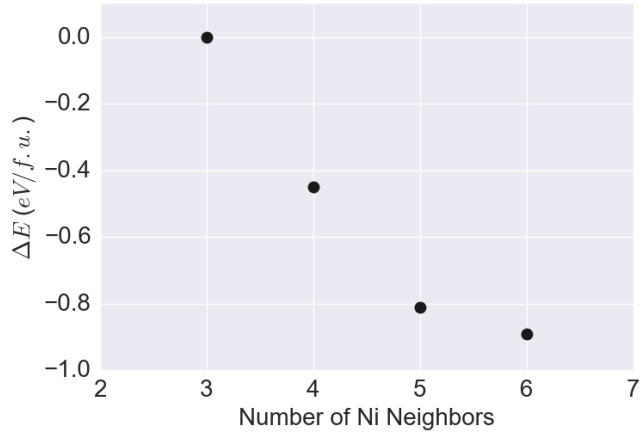

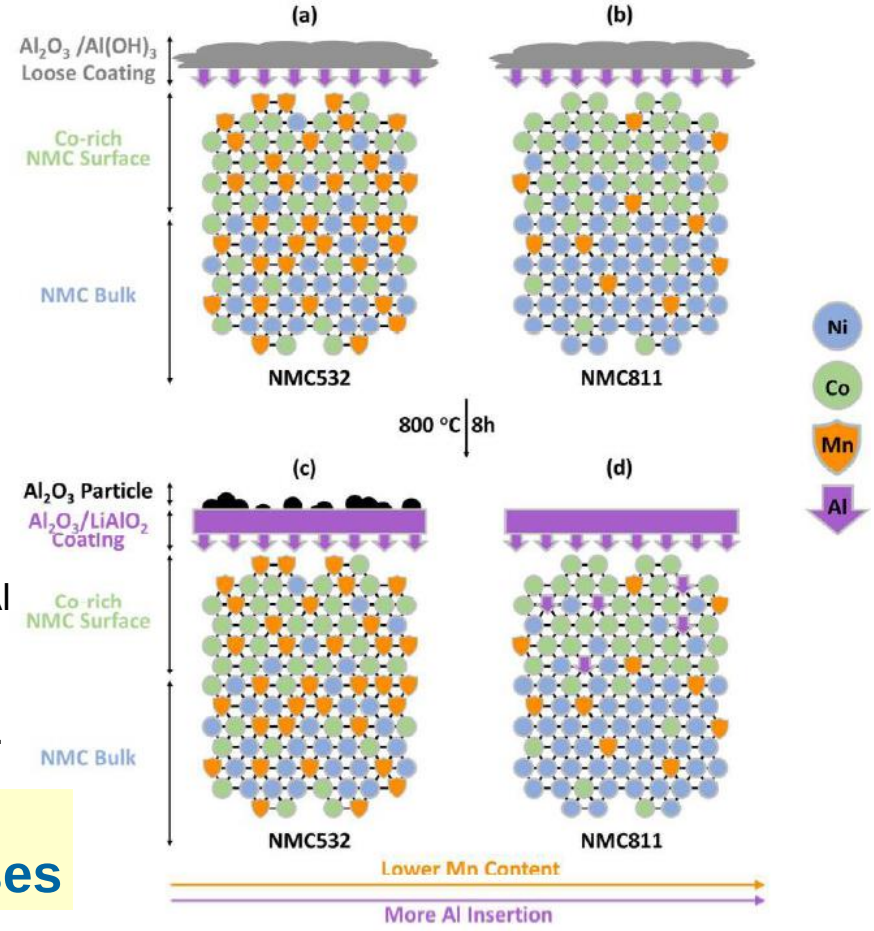

- Swapping Ni and Co in the TM layer changes the Al environment.
- Energy gain with increasing Ni and Co near surface Al is larger than the cost of the exchange (Mn-Al swapping).
- Al prefers to be surrounded by Ni then Co but not Mn.

The energy decreases when the number of Ni neighbors to Al increases

SUMMARY

Atomistic modeling

- Thermodynamic model predicts particle shape, (012) surface most reactive facet, facet-dependent transition metal segregation
- Fluorinated electrolytes present a lower reactivity toward oxidation at the cathode compared to non-fluorinated electrolytes.
- The strength of the interaction of phosphite additives with the cathode surface depends on the functional groups and the degree of decomposition of the additive.
- TMSPi decomposition products passivate the surface of NMC cathodes.
- Complexation of transition metals affects dissolution.
- A thin buffer α-$LiAlO_2$ phase between γ-$LiAlO_2$ and NMC (012) surface is predicted.
- Al dissolved in the cathode induces elemental segregation to the surface.

Electrochemical modeling

- Simple electrode current balance model effective for examining a wide range of cell characteristics affected by side reaction phenomena.
- Existing electrochemical model modified to examine side reactions and crosstalk between electrodes.
- The long time constant for cell current change observed during high voltage potentiostatic holds is generally associated with side reactions. Similarly, most of current goes into the redox of side reactants and not lithium loss.

FUTURE WORK AND WORK IN PROGRESS

Atomistic modeling

- Surface dopants to mitigate dissolution, surface reconstruction, reaction with the electrolyte (descriptors?).
- Surface reconstruction-strain-segregation relationships.
- Effect of surface reconstructions on impedance raise.
- Additional additives-surfaces interactions.
- Solvent and additives decomposition micro-kinetics modeling.

Electrochemical modeling

- Expand model to include impact of transition metal dissolution, oxygen release from oxide surface, and gas generation within cell.
- As side reaction complexity increases, methods for simplifying electrochemical model will be explored.

CONTRIBUTORS AND ACKNOWLEDGMENT

Research Facilities

- Materials Engineering Research Facility (MERF)
- Post-Test Facility (PTF)
- Cell Analysis, Modeling, and Prototyping (CAMP)
- Battery Manufacturing Facility (BMF)
- Advanced Photon Source (APS)
- Argonne Leadership Computing Facility (ALCF)

High-Energy/Voltage Project Contributors

- Daniel Abraham
- Mahalingam Balasubramanian
- Chunmei Ban
- Javier Bareño
- Ira Bloom
- Jiayu Cao
- Guoying Chen
- Pierre Claver
- Jason Croy
- Lamuel David
- Dennis Dees
- Fulya Dogan Key
- Nancy Dudney
- Alison Dunlop
- Juan Garcia
- Binghong Han
- Kevin Hays
- Meinan He
- Katherine Hurst
- Hakim Iddir
- Andrew Jansen
- Christopher Johnson
- Ozge Kahvecioglu Feridun
- Kaushik Kalaga
- Andrew Kercher
- Joel Kirner
- Robert Klie
- Michael Kras
- Gregory Krumdick
- Jianlin Zhu
- Changwook Lee
- Xuemin Li
- Chen Liao
- Qian Liu
- Wenquan Lu
- Anil Mane
- Chengyu Mao
- Jagjit Nanda
- Daniel O'Hanlon
- Cameron Peebles
- Nathan Phillip
- Bryant Polzin
- Yang Ren
- Ritu Sahore
- Youngho Shin
- Ilya Shkrob
- Robert Tenent
- Rose Ruther
- Robert Sacci
- Adam Tornheim
- Stephen Trask
- Marco Tulio
- John Vaughey
- Gabriel Veith
- David Wood
- Zhengcheng Zhang
- Jian Zhu

Support for this work from the ABR Program, Office of Vehicle Technologies, DOE-EERE, is gratefully acknowledged – Peter Faguy, David Howell

RESPONSE TO PREVIOUS YEAR'S REVIEWER COMMENTS

All comments by reviewers were positive last year

- This reviewer praised the approach as excellent. The reviewer pointed out the modeling efforts are combined with experimental studies. The obtained models are used to understand the interactions between cathode surface and electrolyte/additives and the reviewer concluded the results are consistent with the experimental findings and surface analysis.
- The reviewer praised this work for achieving very impressive milestones. The project has had a significant progress in one year the reviewer observed, and the findings can be used as a predictive tool to improve high-energy LIBs.
- This reviewer said excellent collaboration with other teams was evident and needed. The strength(s) of each collaborator was maximized.
- The reviewer acknowledged that the project is very helpful in order to understand electrode bulk and surface structures, processes at surfaces and interfaces, and electrolyte-surface interactions to address the problems associated with "enabling" high-energy Li-ion cells.
- The reviewer pointed out this work can be improved by providing more experimental support for the computational results.

Response – We thank the reviewers for their encouraging remarks on the progress made within the project and will endeavor to incorporate as much experimental collaboration as possible.

TECHNICAL BACKUP SLIDES

Simple Electrode Current Balance Model Utilized to Make Basic Conclusions about Side Reactions

For each electrode, the rate of change in capacity (C_+ and C_-) combined with side reaction current (I_{Oxd} for positive and I_{Red} for negative) is equal to the cell current (I_{Cell}).

$$I_{Cell} = \frac{dC_+}{dt} - I_{Oxd} = -\left(\frac{dC_-}{dt} + I_{Red}\right) \qquad C_{Cell} = C_+ + C_-$$

$$\frac{dC_{Cell}}{dt} = I_{Oxd} - I_{Red}$$

- Positive oxidation side reactions increase cathode capacity (C_+) and negative reduction side reactions decrease anode capacity (C_-).

$$CE = \frac{I_D}{I_C}\frac{I_C - (I_{Red})_{Cavg}}{I_D + (I_{Red})_{Davg}}$$

- If the discharged cell's anode is empty, then the current efficiency (CE) is determined by the cycling currents (I_C for charge and I_D for discharge) and the side reduction current.

$$CE = \frac{I_D}{I_C}\frac{I_C - (I_{Oxd})_{Cavg}}{I_D + (I_{Oxd})_{Davg}}$$

- If the discharged cell's anode contains excess lithium, then the current efficiency is determined by the cycling currents and the side oxidation current.

$$I_{Cell} = -I_{Oxd}$$

- Cell current for NMC//Graphite cells at long times during a potentiostatic hold is equal to the positive oxidation side reaction current, assuming the graphite electrode is in a two-phase region (i.e. flat OCV curve).

Electrochemical Model Used to Examine Potentiostatic Hold Data on Full Cells

4.6 volt hold on NMC//graphite coin cell at room temperature

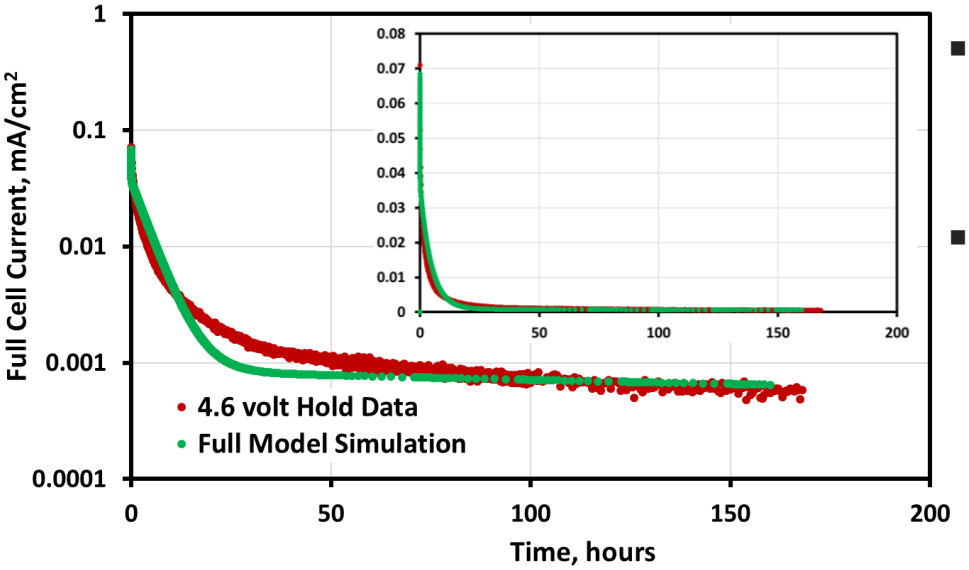

- Time constants associated with the main cell reaction are on the order of hours or less.
- The long time constant for the hold is generally associated with side reactions.
  - Slow change in R and R^+ concentrations.
  - SEI (i.e. F) growth on the positive.

- Multiple side reactions needed to improve fit.
- SEI generation reactions at least an order of magnitude lower than main crosstalk reactions.
- Most of current goes into redox of side reactants (i.e. R crosstalk reactions) and not lithium loss.
- Corresponding small change in cyclable lithium.

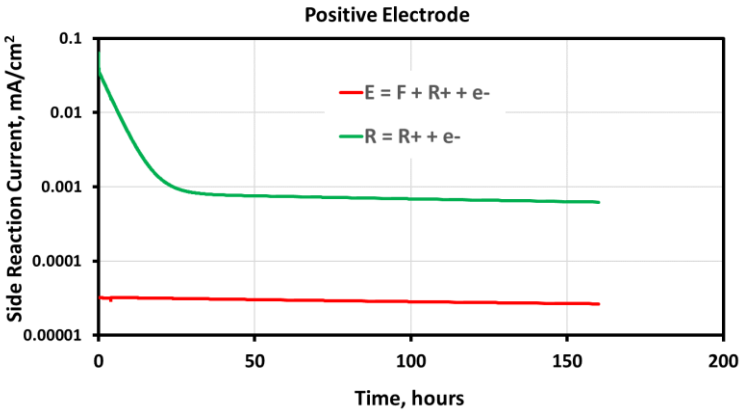

TMSPI DECOMPOSITION

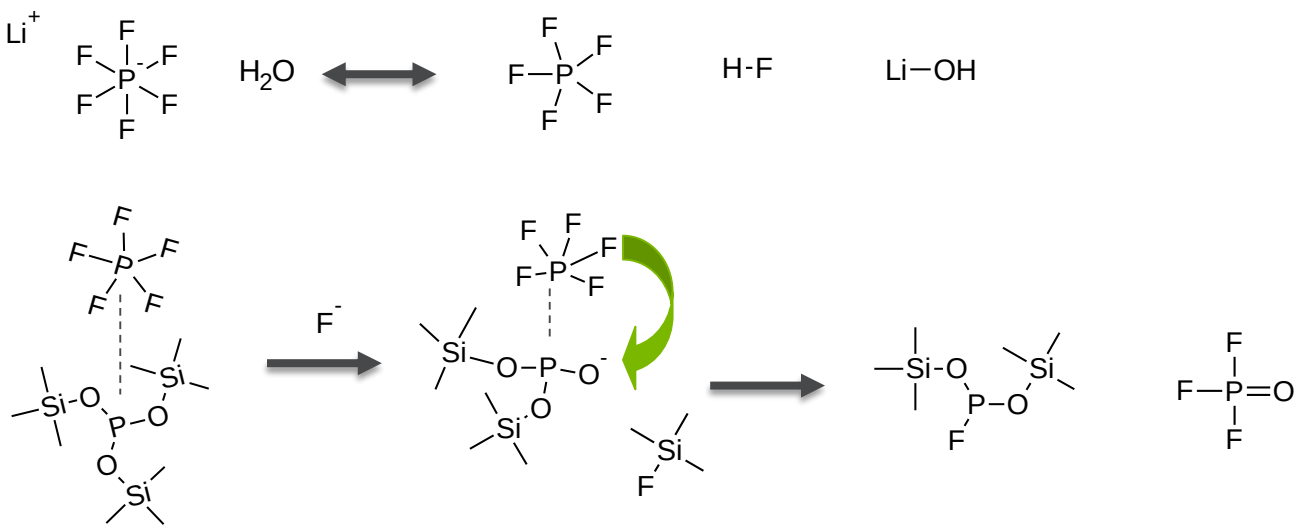

Stable intermediate

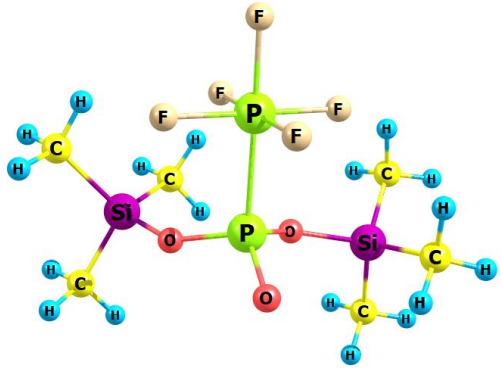

- The actual decomposition mechanism may involve HF and PF_5.
- Intermediates have been found experimentally (NMR) and theoretically (DFT).

TMSPI DECOMPOSITION TIMELINE

E = 0.0eV E = -0.15eV E = -0.25eV E = -0.58eV

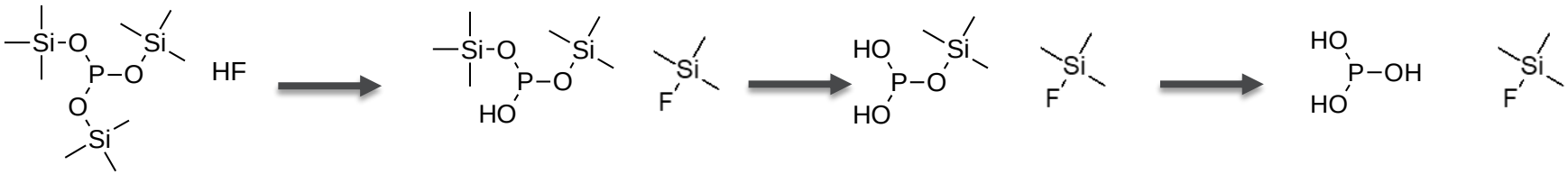

E = 0.0eV E = -1.15eV E = -0.07eV E = 0.11eV

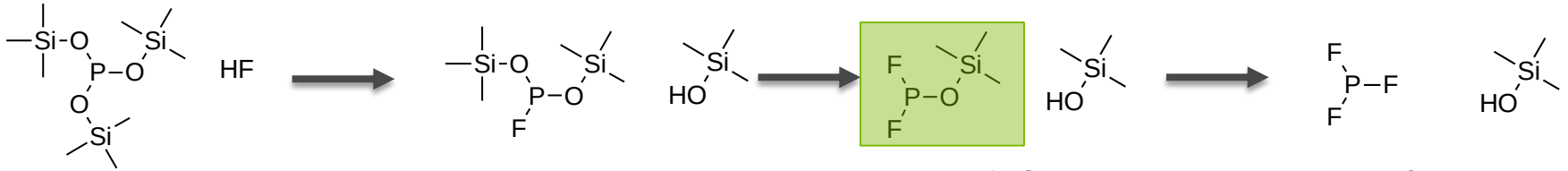

E = 0.0eV E = -1.0eV E = -1.8eV E = -2.5eV

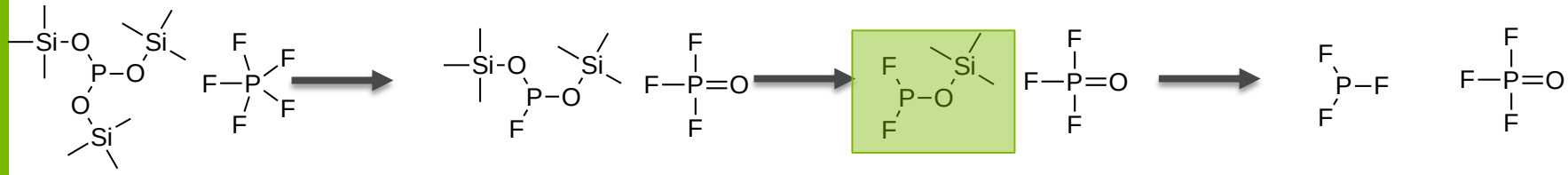

- TMSPi reaction with HF is thermodynamically favorable.
- Further decomposition goes trough PF_3 route preferentially.
- Reaction with PF_5 is favored after the first decomposition step.

SURFACE PASSIVATION MECHANISM

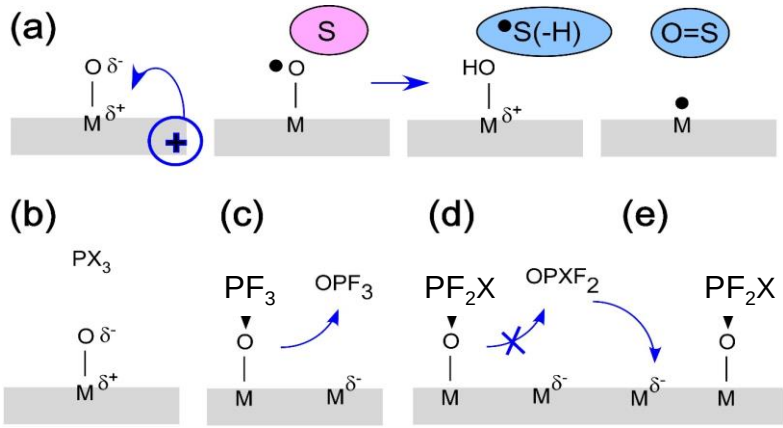

(a) oxidation of the solvent by charged M-O reaction centers on the cathode surface

(b) No interaction.

(c) PF_3 oxidation via oxygen removal from the surface.

(d-e) PF_2X binds to the surface.

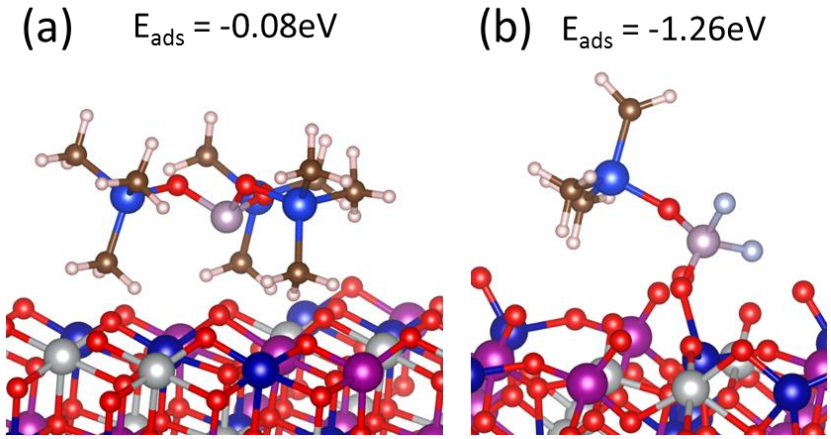

Molecular configuration for chemisorbed (a) PX3 and (b) PF2X molecules on partially delithiated NMC.

- The phosphate formed at the surface is less prone to lose a OTMS group.
- TMSPi (PX_3) has a weak interaction with the surface while PF_2X (1 branch) molecules interact strongly with the surface (chemisorption, surface passivation).

Methodology for Electrochemical Model

Combines thermodynamic and interfacial effects with continuum based transport equations

Bulk Solid-State Diffusion

$$\frac{\partial c_{Sb}}{\partial t} = \frac{\partial}{\partial z}\left(D_{Sb}\frac{\partial c_{Sb}}{\partial z}\right)$$

Transport, Reaction, and SEI Growth of Side Reaction Components

$$i_n = i_0\left\{\exp\left[\frac{\alpha_A F}{RT}\left(\Phi_1 - \Phi_2 - U - \eta_c\right)\right] - \exp\left[-\frac{\alpha_C F}{RT}\left(\Phi_1 - \Phi_2 - U - \eta_c\right)\right]\right\}$$

$$\frac{\sum i_n}{z_i F} = -D_i\frac{c_{iE} - c_{iS}}{\delta_{SEI}} \qquad \eta_c = \frac{RT}{nF}\sum_i s_i \ln\frac{c_{iE}}{c_{iS}} \qquad \sum_i s_i M_i^{z_i} \leftrightarrow ne^-$$

$$\frac{d\delta_{SEI}}{dt} = \frac{\sum i_n V_{SEI}}{F} \qquad \frac{\partial \varepsilon c_i}{\partial t} = \nabla\cdot\left(\frac{\varepsilon D_i}{\tau}\nabla c_i\right) + a\sum j_n$$

Transport through Cell Sandwich

$$\varepsilon\frac{\partial c}{\partial t} = \frac{\varepsilon}{\tau}\frac{\partial}{\partial x}\left(D\frac{\partial c}{\partial x}\right) + \frac{1}{z_+\nu_+ F}\frac{\partial\left[\left(1 - c\bar{V}_e\right)\left(1 - t_+^o\right)i_2\right]}{\partial x}$$

$$i_2 = -\frac{\kappa\varepsilon}{\tau}\frac{\partial\Phi_2}{\partial x} - \nu RT\frac{\kappa\varepsilon}{F\tau}\left(\frac{s_+}{n\nu_+} + \frac{t_+^o}{z_+\nu_+}\right)\left(1 + \frac{\partial \ln f_\pm}{\partial \ln c}\right)\frac{1}{c}\frac{\partial c}{\partial x}$$

$$\frac{\partial i_2}{\partial x} = Fz_+\sum_k a_k j_{kn} \qquad I = i_1 + i_2 \qquad i_1 = -\sigma_{eff}\frac{\partial\Phi_1}{\partial x}$$

- Side reaction components diffuse between electrodes and through SEI from electrolyte where they react with electrons diffusing from the solid conductors. Initially the reaction front assumed to be narrow and close to solid.
- All electrolyte components from side reactions are considered minor constituents.
- Volume averaged transport equations account for the composite electrode geometry.
- The system of partial differential equations are solved numerically to obtain concentration, potential, and current distributions throughout cell.

Description of original model in *Journal of The Electrochemical Society*, **155** (8) A603 (2008)

Initial Electrochemical Model Developed Based on Generic Side Reaction Mechanism

Initial rate limitation (i.e. kinetics, diffusion, or combination) for side reactions based on known or estimated reaction potentials

Negative: $xLi^+ + xe^- + \theta \leftrightarrow Li_x\theta$ Main electrochemical reaction

E°=0.8v, Diffusion $Li^+ + e^- + E \leftrightarrow SEI$

E°=2.0v, Diffusion $e^- + R^+ \leftrightarrow R$

E°=0.2v, Kinetics $Li^+ + e^- + R \leftrightarrow SEI$

} Reduction side reactions

Positive: $Li_y\theta \leftrightarrow yLi^+ + ye^- + \theta$ Main electrochemical reaction

E°=3.7v, Kinetics and/or Diffusion $E \leftrightarrow F + R^+ + e^-$

E°=2.0v, Diffusion $R \leftrightarrow R^+ + e^-$

} Oxidation side reactions

- Model includes reduction and oxidation of electrolyte solvent specie (E) and reacted solvent specie (R), as well as crosstalk between electrodes.
- In actuality each side reaction is likely a complex matrix of reactants and products that probably occur over a range of potentials.
  - R is actually R_1, R_2, R_3,…

Description of reaction mechanism in *Journal of The Electrochemical Society*, **164** (2) A508 (2017)